CHEMISTRY
A EUROPEAN JOURNAL

ChemPubSoc
Europe

DOI: 10.1002/chem.201203914

Three-Dimensional MOF-Type Architectures with Tetravalent Uranium Hexanuclear Motifs (U_6O_8)

Clément Falaise, Christophe Volkringer, Jean-François Vigier, Natacha Henry, Arnaud Beaurain, and Thierry Loiseau*[a]

Abstract: Four metal–organic frameworks (MOF) with tetravalent uranium have been solvothermally synthesized by treating UCl_4 with rigid dicarboxylate linkers in *N*,*N*-dimethylfomamide (DMF). The use of the ditopic ligands 4,4′-biphenyldicarboxylate (**1**), 2,6-naphthalenedicarboxylate (**2**), terephthalate (**3**), and fumarate (**4**) resulted in the formation of three-dimensional networks based on the hexanuclear uranium-centered motif $[U_6O_4(OH)_4(H_2O)_6]$. This motif corresponds to an octahedral configuration of uranium nodes and is also known for thorium in crystalline solids. The atomic arrangement of this specific building unit with organic linkers is similar to that found in the zirconium-based porous compounds of the UiO-66/67 series. The structure of $[U_6O_4(OH)_4(H_2O)_6(L)_6]\cdot X$ (L = dicarboxylate ligand; X = DMF) shows the inorganic hexamers connected in a face-centered cubic manner through the ditopic linkers to build up a three-dimensional framework that delimits octahedral (from 5.4 Å for **4** up to 14.0 Å for **1**) and tetrahedral cavities. The four compounds have been characterized by using single-crystal X-ray diffraction analysis (or powder diffraction analysis for **4**). The tetravalent state of uranium has been examined by using XPS and solid-state UV/Vis analyses. The measurement of the Brunauer–Emmett–Teller surface area indicated very low values (Langmuir $<300\ m^2g^{-1}$ for **1**, $<7\ m^2g^{-1}$ for **2**–**4**) and showed that the structures are quite unstable upon removal of the encapsulated DMF solvent.

Keywords: dicarboxylic acids · metal–organic frameworks · photoelectron spectroscopy · solvothermal synthesis · uranium · X-ray diffraction

Introduction

The chemistry of actinide metals is very rich and exhibits diverse crystalline atomic arrangements of molecular species or infinite extended networks partly driven by the wide range of oxidation states (from 3+ up to 7+). One of the most studied elements is uranium because of its use as a fuel in nuclear industry. Although the hexavalent form (uranyl cation, $[UO_2]^{2+}$) is the most stable oxidation state under ambient conditions and is encountered in most natural minerals,[1] nuclear reactors commonly use ceramic uranium dioxide, UO_2, which corresponds to the tetravalent form. Considering the chemical processing for separation and purification of uranium from spent nuclear fuel, the oxalate route has been intensively investigated, which gave rise to dedicated studies of the interactions of this particular ditopic ligand with tetravalent uranium in nitric solution. In this context, the crystallization and isolation of oxalate uranium(IV) phases have been examined and are known to lead to different compositions that also incorporate hetero elements.[2] More generally, the reactivity of carboxylates with hexavalent uranium has been very well explored. Over the last decade, a large number of contributions have been reported structural descriptions of the so-called uranyl–organic frameworks (UOFs),[3] which follow the idea developed for the generation of metal–organic frameworks (MOFs).[4] In this area, the strategy relies on the choice of aliphatic or aromatic carboxylate ligands, which may have multidentate O-donor (and N-donor) functions that chelate or/and bridge the uranyl cations to form extended coordination polymers with different dimensionalities (1D, 2D, or 3D). In contrast, available structural data for tetravalent uranium in association with carboxylate ligands (other than oxalates) are quite rare, which is partly due to the difficulty of stabilizing the low valent states of uranium in an ambient air atmosphere. The synthesis of uranium(IV) carboxylates was first reported in the 1960s,[5] but this research domain has been renewed quite recently with the identification of discrete molecular oxo/hydroxo polynuclear entities in which the numbers of uranium centers vary from 1 to 16.[6] The role of the water content in the organic solvent medium was found to be crucial for the hydrolysis rate of the condensation process, leading to the formation of molecular assemblies of large and well-defined polymeric species

[a] C. Falaise, Dr. C. Volkringer, Dr. J.-F. Vigier, Dr. N. Henry, Dr. A. Beaurain, Dr. T. Loiseau
Unité de Catalyse et Chimie du Solide (UCCS)
UMR CNRS 8181, Université de Lille Nord de France
USTL-ENSCL, Bat C7, BP 90108
59652 Villeneuve d'Ascq (France)
Fax: (+33) 320-43-48-95
E-mail: thierry.loiseau@ensc-lille.fr

Supporting information for this article is available on the WWW under http://dx.doi.org/10.1002/chem.201203914.

U_6,[6c,d,7] U_{10},[6e] U_{12},[7] or U_{16}.[6e] In these different examples, the polyoxo clusters are stabilized by peripheral monodentate ligands, such as formate, triflate, or benzoate groups. To design frameworks based on interconnected uranium-based motifs, we initiated investigations using polydentate carboxylate linkers, such as the trimesate group. With this particular molecule, we recently reported the first three-dimensional framework based on uranium(IV) cations, which interact with these tritopic molecules to generate a channel-like open structure.[8]

Herein, we systematically explore the solvothermal reactivity of linear ditopic molecules, such as terephthalate, 2,6-naphthalendicarboxylate, 4,4′-biphenyldicarboxylate, and fumarate, with low valent uranium(IV) cations in *N*,*N*-dimethylformamide solvent. Four compounds with uranium(IV) that are closely related to the zirconium-based porous coordination polymers of UiO-66[9] have thus been prepared and structurally characterized. Spectroscopic analyses (XPS, UV/Vis) and estimations of surface area have been carried out.

Results and Discussion

Four MOF-type compounds **1**–**4** of tetravalent uranium with aromatic dicarboxylate linkers 4,4′-biphenyldicarboxylate (4,4′-bpdc; **1**), 2,6-naphthalenedicarboxylate (2,6-ndc; **2**), 1,4-benzenedicarboxylate (1,4-bdc; **3**), or fumarate (fum; **4**) have been isolated. They have been obtained by solvothermal treatment of uranium chloride (UCl_4) with ditopic acids (HO_2C-R-CO_2H, R = benzene, biphenyl, naphthalene, or HC=CH groups) in *N*,*N*-dimethylformamide together with a controlled amount of water (30 μL; 1.67 mmol). These phases exhibit a three-dimensional atomic arrangement that consists of the same hexanuclear uranium-centered building blocks connected to each other by the ditopic organic carboxylates and corresponding to a chemical composition $[U_6O_4(OH)_4(H_2O)_6(L)_6]\cdot X$ (L = 4,4′-bpdc, 1,4-bdc, 2,6-ndc, or fum; X = solvent). The resulting frameworks are similar to those found for tetravalent zirconium UiO-66 (with 1,4-bdc), UiO-67 (with 4,4′-bpdc),[9] or with fumarate.[10] The structures of compounds **1**–**3** have been determined from single-crystal XRD analysis, whereas the cell parameters and structural model of **4** were obtained from the powder XRD pattern data due to the small size of the crystallites. All the compounds crystallize in a cubic cell with a = 27.4526(9) Å for **1**, a = 24.5681(1) Å for **2**, a = 21.5151(11) Å for **3**, and a = 18.75518(8) Å for **4**, but different space groups were observed for each because the locations of the dicarboxylate linker induce some lower symmetries, as previously reported in the literature.[10] The crystal structures are built from six uranium cations lying in one crystallographically independent site in **1**–**3** and two sites in **4**. These cations are coordinated to nine oxo, hydroxo, or aquo groups, which define a monocapped square anti-prismatic geometry (Figure 1). The uranium centers are located in such a way that they occupy each corner of an ideal octahedral core (O_h point symmetry). Four of the oxygen atoms belong to one square plane and are linked to three uranium atoms, which gives rise to an edge-sharing connection mode between the UO_9 polyhedra. Regarding the electroneutrality of the structure, half of the oxygen atoms are μ_3-oxo groups and half are μ_3-hydroxo groups. Four other oxygen atoms are located at each corner of the second square plane of the anti prism and belong to the carboxylate arms of the organic molecules (U−O3 2.318(11) Å for **1**; U−O11,12 2.382(7)–86(8) Å for **2**; U−O11 2.367(6) Å for **3**). The remaining oxygen atom is in a terminal position and is assigned to a water molecule that caps one square plane of the anti-prism (U−Ow 2.70(4) Å for **1**; U−Ow 2.6705(11) Å for **2**; U−Ow 2.657(17) Å for **3**). This super-octahedral building block has been reported for tetravalent uranium several times in the literature. First described with sulfates[11] or phosphonates,[12] it was then encountered in different coordination complexes as discrete entities involving organic ligands, such as triflate,[7,13] formate,[6c] or benzoate[6d] molecules. Due to the high symmetry of the cubic framework ($Fm\bar{3}m$ for **1** and **3** or derived space groups $F23$ for **2** and $P23$ for **4**), distinguishing the μ_3-O or μ_3-OH ligands from the U−O bonds is rather difficult (by XRD analysis) because only average U−O or U−OH lengths are observed. In **1** and **3** (from single-crystal structure determination), the U−(μ_3-O) bonds are 2.332(12) Å for **1** and 2.314(9) Å for **3**, which correspond to an average value between the U−OH bond (2.40–

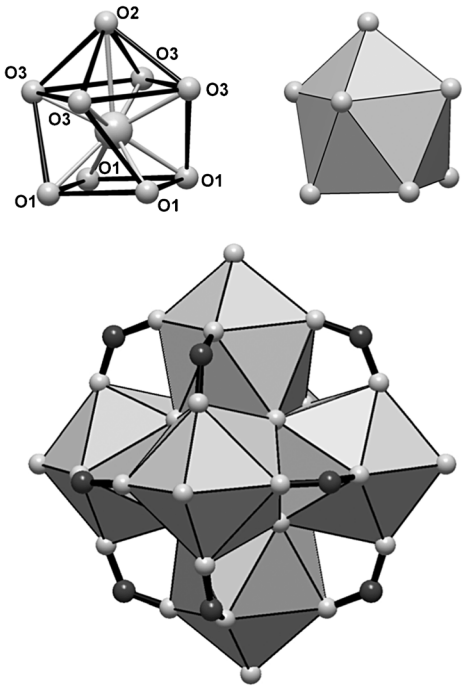

Figure 1. Top: Coordination environment around the tetravalent uranium cation (central atom), defining a monocapped square anti-prism polyhedron $[U_6O_4(\mu_3\text{-}O)_2(\mu_3\text{-}OH)_2(H_2O)_6]$. Bottom: Polyhedral representation of the hexanuclear uranium-centered core. One illustration of the atomic labels is given for the ninefold coordinated uranium in $[U_6O_4(OH)_4(H_2O)_6(L)_6]$ (L = 4,4′-bpdc, **1**). Each uranium center is located at the corner of an octahedral polyhedron. O1 is the μ_3-oxo or μ_3-hydroxo group. O3 is a carboxyl oxygen. O2 is a terminal water molecule.

2.50 Å)[6c,d] and the U−O bond (2.20–2.27 Å)[6c,d,7,13] previously observed for hexanuclear blocks that have been described in lower symmetry. Indeed, in the highly symmetrical uranium sulfate,[11] the average value for the U−O,OH bond is 2.367 Å. In compounds **1** and **3**, the O or OH species are delocalized on the μ_3 nodes because they are structurally equivalent. However, the structure of **2** is described with a distinct space group (*F*23) and two sets of contrasted U−O bond lengths are observed with values of 2.225(6) or 2.390(6) Å, which would indicate the occurrence of μ_3-oxo and μ_3-hydroxo groups, respectively. Such a discussion comparing the U−O bonds in compound **4** is quite delicate because the powder XRD data (from a conventional source) are not accurate enough for a proper interpretation. The oxidation state of uranium, which may be questionable in this type of coordination compound,[6e,7] has been analyzed by X-ray photoelectron spectroscopy (XPS) analysis (Figure 2, Figure S8 in the Supporting Information). The U4f XPS spectra shows two sets of binding energies in the range of 380.2 to 380.7 and 391.1 to 391.6 eV, which correspond to the $U4f_{7/2}$ and $U4f_{5/2}$ components, respectively. These binding energy values and their satellite shifts (+6.4—6.8 eV) are similar to those observed in uranium(IV) trimesate[8] or other tetravalent uranium compounds previously reported in the literature.[14] Solid-state UV/Vis spectra (Figure 2, Figure S9 in the Supporting Information) of the different samples show a broad signal in the range of $\lambda = 600$ to 700 nm, which was assigned to the $^3H_4 \rightarrow {}^3P_0$, $^3H_4 \rightarrow {}^1G_4$, and $^3H_4 \rightarrow {}^1D_2$ transitions and also characterizes the tetravalent state of uranium.[15]

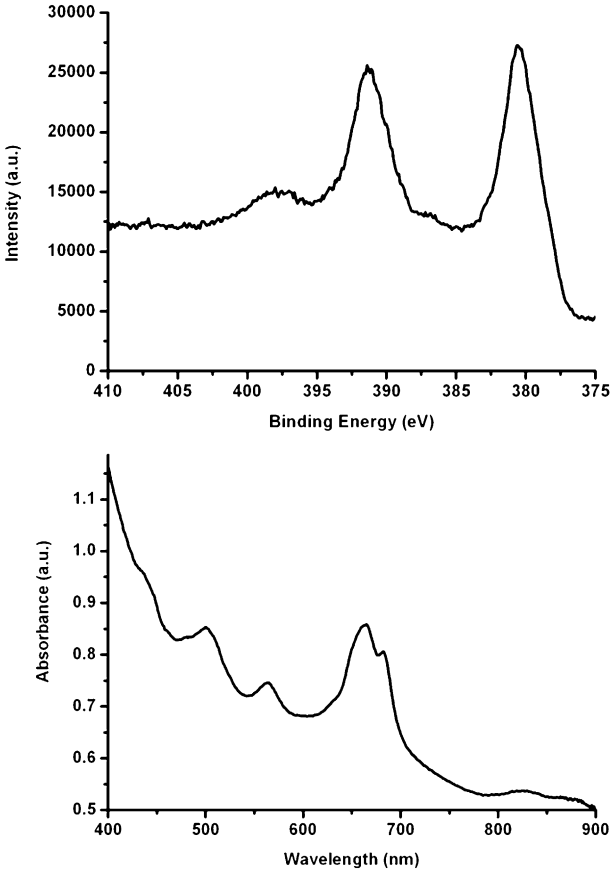

Figure 2. Top: XPS spectrum and bottom: UV/Vis spectrum of $[U_6O_4(OH)_4(H_2O)_6(4,4'\text{-bpdc})_6]\cdot 14\,DMF$ (**1**).

These hexanuclear $[U_6O_4(OH)_4(H_2O)_6]$ cores are connected to each other through twelve ditopic ligands, which act as *syn–syn* bidentate bridging linkers with four uranium centers. The aromatic ring of the dicarboxylate linkers is found to be statistically disordered over two equivalent positions for compounds **1** and **2** (see Figure S4 in the Supporting Information). This situation did not change when the XRD intensity was measured at low temperature (100 K for **1**). This bidentate connection results in a face-centered cubic lattice of hexamers and generates a three-dimensional system of cavities delimited by $[U_6O_4(OH)_4(H_2O)_6]$ nodes with octahedral and tetrahedral symmetries (Figure 3). Within the cubic cell, the arrangement of these two geometrical types of voids is identical to that observed in the dense archetypal phases of NaCl (rock salt) or ZnS (blende) with fcc packing. This type of connection was illustrated by zirconium in a series of isoreticular porous coordination polymers built on the closely related $Zr_6O_4(OH)_4$ clusters linked through dif-

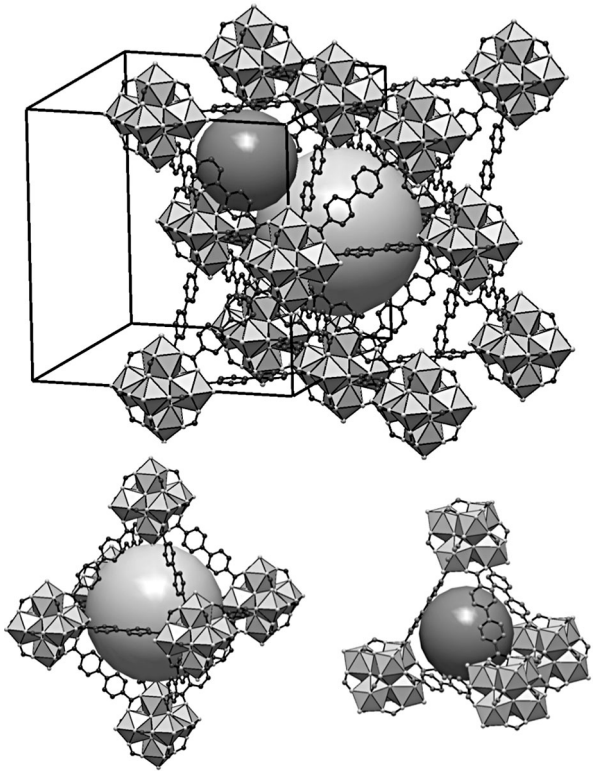

Figure 3. Representation of the connection of the hexameric $[U_6O_4(\mu_3\text{-}O)_2(\mu_3\text{-}OH)_2(H_2O)_6]$ building units that generate a cubic arrangement (face-centered cubic or fcc) delimiting octahedral cavities (light gray sphere) and tetrahedral cavities (dark gray sphere). This type of topology was previously referred to as UiO-67 (with 4,4′-bpdc) or UiO-66 (with 1,4-bdc) with zirconium. The structure of compound **1** (with 4,4′-bpdc) is presented here and disordering of the benzene ring of the organic ligand is not shown for clarity.

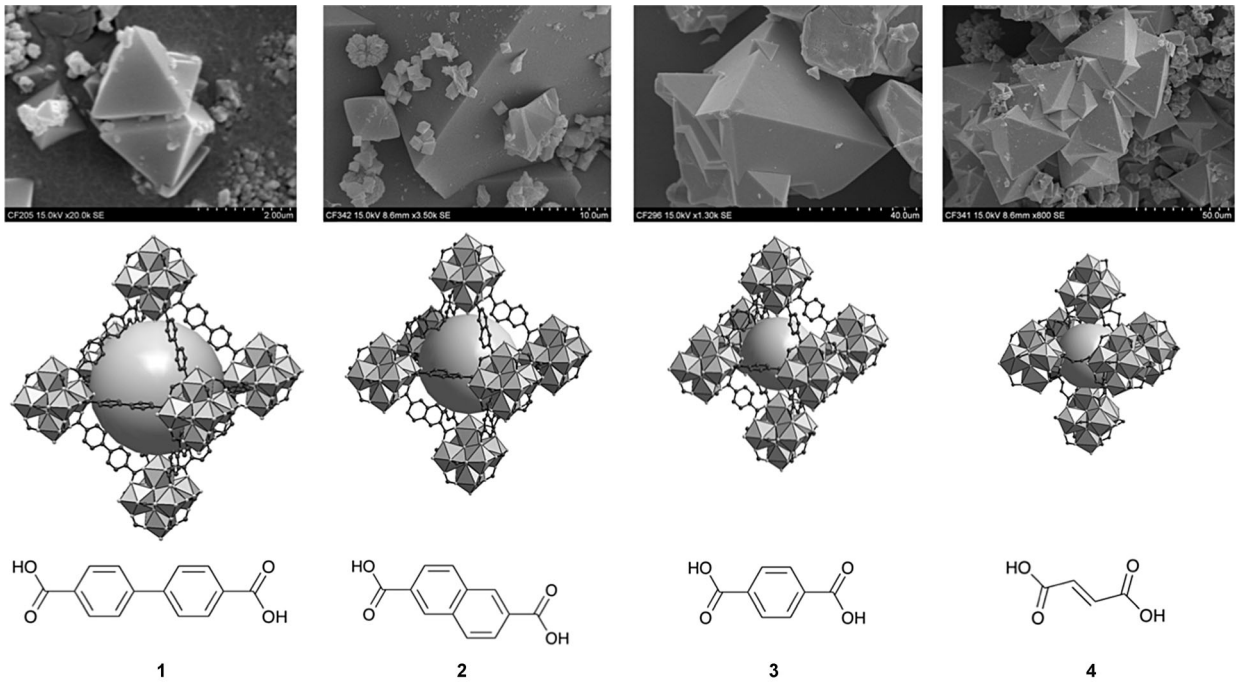

Figure 4. Top: SEM images of compounds $[U_6O_4(OH)_4(H_2O)_6(L)_6]\cdot x$DMF; scale bars: 2 μm, 10 μm, 40 μm, 50 μm for **1**, **2**, **3**, and **4**, respectively. Bottom: Evolution of the size of the octahedral cavity in the series $[U_6O_4(OH)_4(H_2O)_6(L)_6]\cdot x$DMF; from left to right: L = 4,4′-bpdc (**1**), 2,6-ndc (**2**), 1,4-bdc (**3**), and fum (**4**).

ferent linear ditopic ligands, such as terephthalate (UiO-66),[9,16] 4,4′-biphenyldicarboxylate (UiO-67),[9,17] terphenyldicarboxylate (UiO-68),[9] and their NH_2-derived ligands[18] azobenzenedicarboxylate,[19] *trans*-muconate,[17] or fumarate.[10] For these different compounds, the size of the octahedral and tetrahedral voids is directly correlated to the length of the linear dicarboxylate molecules and can reach, for example, a value of 25.6 Å (octahedral pore) in UiO-68.[18] The hexanuclear unit $[Zr_6O_4(OH)_4]$ was recently involved in the construction of different topologies that offer large cavity diameters.[20] In our uranium-based compounds, the estimated pore sizes of the octahedral voids (based on an ionic radius of 1.35 Å for oxygen) are 14.0, 11.1, 8.1, and 5.4 Å for **1**, **2**, **3**, and **4**, respectively (Figure 4). The XRD analysis did not reveal any clear evidence of the nature of the encapsulated molecules within these cavities, but one may assume the presence of trapped DMF molecules. From the elemental chemical analyses, we found that the amount of DMF species decreases with the size of cavities. Infrared spectroscopy (see Figure S7 in the Supporting Information) also confirms the presence of DMF, with a doublet at around 2900 cm^{-1} ($\nu_{O=C-H}$) and the vibration band at 1656 cm^{-1} ($\nu_{C=O}$). The broad band centered in the range of 3500 to 3300 cm^{-1} is characteristic of hydrogen bonds between species such as bonded hydroxyl groups, water, or trapped DMF.

Moreover, the parent UiO-66-type structure containing the 2,6-naphthalenedicarboxylate group (phase **2** in our work) has not been isolated with zirconium up to now and constitutes a new member of this topological series. For uranium, the incorporation of such hexanuclear cores in coordination polymers that form extended networks through the use of ditopic ligands is quite new because only discrete molecular species have been previously reported in the literature.[6c,d,7,13] In fact, this situation exists in the first example of $[U_6O_4(OH)_4]$ units linked to each other through $[SO_4]$ groups.[11] It represents a dense, purely inorganic uranium sulfate, which was obtained by crystallization from aqueous solvent. Considering this specific coordination chemistry with tetravalent heavy metals, similar isolated molecular hexanuclear clusters have been previously reported for crystal structures with zirconium,[21] cerium,[22] and also with thorium. Thorium can be stabilized by monotopic carboxylate linkers by forming similar discrete hexanuclear $[Th_6O_4(OH)_4]$ blocks.[6c,23] Note that other polyoxo U_6 cores have been identified with μ_2-oxo connection configurations, such as Lindqvist[24] or ring-based clusters.[25] Another illustration of an actinide-based hexanuclear core has been recently observed in solution for neptunium(IV) stabilized by formate groups.[26]

The different compounds were analyzed by thermogravimetric analysis (see Figure S5 in the Supporting Information), which showed quite similar thermal behavior for **1**–**3**. Under an air atmosphere, a continuous weight loss was observed from room temperature up to 400 °C, followed by a second event up to 410 °C for **1** and **2** and up to 430 °C for **3**. These two events could be successively assigned to the evacuation of the trapped DMF molecules and the degradation of the organic linkers. Based on the final composition, U_3O_8, the observed remaining weight values are 44.7 % (calcd: 40.8 %) for phase **1**, 43.1 % (calcd: 43.2 %) for phase **2**, and 51.6 % (calcd: 49.8 %) for phase **3**. The thermogravimetric

curve of compound **4** is slightly different because a first weight loss (5.6%) was observed up to 80°C, followed by a plateau up to 200°C. This could correspond to the departure of approximately two encapsulated DMF molecules per U_6O_8 unit (calcd: 5.4%). Between 200 and 500°C, a quite slow and continuous weight loss was observed. The final remaining weight is 60.8% and agrees well with the theoretical value for U_3O_8 (calcd: 62.5%).

The X-ray thermodiffraction experiment (Figure 5, Figure S6 in the Supporting Information) showed that the Bragg peaks of the different phases are clearly visible up to 120°C for **1** and **2** and 140°C for **3** and **4**. The thermal evolution of the powder XRD patterns indicated a structural transformation into amorphous phases for **2**, **3**, and **4**, whereas the broad Bragg peaks of the initial phase persisted for phase **1**. At higher temperature, crystallization of the uranium oxide α-U_3O_8 (pdf file: 47-1493) was observed, and appeared at 360, 380, 400, and 420°C for compounds **1**, **2**, **3**, and **4**, respectively. It was interesting to note that the temperature value of U_3O_8 crystallization increases when the number of carbons from the linker decreases. From these observations, it was surprising to note that compound **1** (with the longest and also the most flexible ligand) is more thermally stable than the other analogues of the UiO-66 parent series.

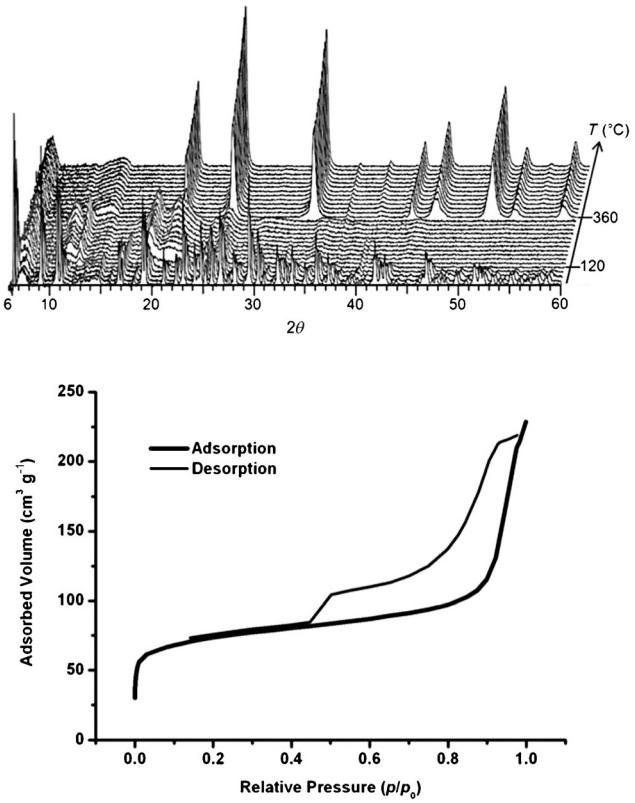

Figure 5. Top: X-ray thermodiffraction patterns ($Cu_{K\alpha}$ radiation, air atmosphere) and bottom: BET curve of $[U_6O_4(OH)_4(H_2O)_6(4,4'\text{-bpdc})_6]\cdot 14\,DMF$ (**1**).

Indeed, this point was correlated to the tentative measurements of porosity, which was estimated by performing a gas sorption isotherm experiment in liquid nitrogen by using a Micromeritics ASAP2010 apparatus. The removal of the trapped species from the as-synthesized phases was found to be quite delicate because washing with solvent (e.g., with chloroform) was not a successful way to get materials with empty pores. Thus, the nitrogen sorption experiment was carried out on samples **1**–**4** (initially stored in a glovebox under Ar) that were degassed at 80°C overnight under primary vacuum. Only compound **1** revealed a type IV isotherm with a hysteresis upon desorption, which is characteristic of a porous solid (Figure 5). The measured Brunauer–Emmett–Teller (BET) surface area was 254(2) $m^2 g^{-1}$ and, assuming a monolayer coverage by nitrogen, the Langmuir surface area was 342(2) $m^2 g^{-1}$. For the other samples, the BET surface area values were measured to be lower than 7 $m^2 g^{-1}$ and indicated the collapse of the three-dimensional framework upon removal of the trapped species. These results are quite disappointing when considering the thermal behavior and high BET surface values reported for the parent zirconium UiO-66-type series. For instance, the Langmuir surface areas of Zr-UiO-66 (L = 1,4-bdc) or Zr-UiO-67 (L = 4,4′-bpdc) were 1187 to 1400[9,18] or 3000 $m^2 g^{-1}$,[9,18] respectively.

Conclusion

This contribution dealt with the second illustration of extended infinite networks that contain tetravalent uranium cations linked to each other through carboxylate linkers. The first example of such MOF-type connection was observed with the isolation of one-dimensional channel frameworks with trinuclear uranium-centered units linked by trimesate ligand.[8] Here, the use of rigid ditopic carboxylate ligands that contained an aromatic ring (terephthalate, 2,6-naphathalenedicarboxylate, 4,4′-biphenyldicarboxylate) or alkene group (fumarate) led to the formation of three-dimensional structures based on a hexanuclear $[U_6O_4(OH)_4(H_2O)_6]$ motif with an octahedral configuration of uranium centers. The arrangement of this specific building unit generates an open framework that delimits octahedral and tetrahedral cavities similar to those previously described for zirconium cations in the UiO-66[9] series of compounds. As expected, the size of the pores is correlated to the length of the ligand, which may be as long as 14 Å when using the 4,4′-biphenyldicarbylate molecule and as short as 5.4 Å for the fumarate molecule. However, the measured accessible BET surface area values were very low compared with those observed for the zirconium series and indicated the difficulty of maintaining the integrity of the three-dimensional framework upon removal of the trapped species in the case of tetravalent uranium. Nevertheless, this work opens the way to the formation of other compounds of UiO-66 type that incorporate other tetravalent heavy atoms, such as thorium(IV)[6c,23] or cerium(IV),[22] for which identi-

cal hexameric units with monocarboxylate ligands have already been encountered in crystalline molecular assemblies.

Experimental Section

Synthesis: Caution! Uranium chloride (UCl_4) is a radioactive and chemically toxic reactant; suitable precautions, care, and protection for the handling of such substances should be followed.

The starting chemical reactants were uranium tetrachloride (UCl_4), 1,4-benzenedicarboxylate ($C_8H_6O_4$, 1,4-H_2bdc, Aldrich, 98%), 4,4′-biphenyldicarboxylate ($C_{14}H_{10}O_4$, 4,4′-H_2bpdc, Aldrich, 97%), 2,6-naphthalendicarboxylic acid ($C_{12}H_8O_4$, 2,6-H_2ndc, Aldrich, 99%), fumaric acid ($C_4H_4O_4$, H_2fum, Aldrich, 99%), and anhydrous *N*,*N*′-dimethylformamide (C_3H_7NO, DMF, Aldrich, 99.8%). The starting chemical reactants (except UCl_4) are commercially available and were used without any further purification. UCl_4 was obtained by using the procedure described in the literature[8] (see the Supporting Information), by using uranium oxide (UO_3, Prolabo Rectapur) and hexachloropropene (Aldrich, 96%). All the reactants were manipulated, weighed, and mixed in a 23 mL Teflon cell under an Ar atmosphere in a glovebox. They were then placed in a closed stainless steel PARR autoclave (type 4746), which was removed from the glovebox and then heated in a conventional electrical oven.

Compound 1: $[U_6O_4(OH)_4(H_2O)_6(4,4'\text{-bpdc})_6]\cdot 14\,DMF$ (**1**) was obtained by a solvothermal reaction in which a mixture of UCl_4 (0.1 g, 0.26 mmol), 4,4′-H_2bpdc (0.063 g, 0.26 mmol), and H_2O (30 μL, 1.67 mmol) in DMF (4 mL, 51 mmol) was heated at 130 °C for 36 h. The resulting green powder was then filtered off, washed with DMF, and dried at RT in an air atmosphere. The product was stable in air for 1 d. Compound **1** was analyzed by using a scanning electron microscope (Hitachi S-3400N) and shows typical octahedrally shaped crystals with a size of 5–10 μm (see Figure S1 in the Supporting Information). Elemental analysis calcd (%) for $C_{126}H_{162}O_{52}N_{14}U_6$: C 36.6, N 4.7, H 3.9; found: C 36.8, N 4.4, H 4.2.

Compound 2: $[U_6O_4(OH)_4(H_2O)_6(2,6\text{-ndc})_6]\cdot 13\,DMF$ (**2**) was obtained by a solvothermal reaction in which a mixture of UCl_4 (0.1 g, 0.26 mmol), 2,6-H_2ndc (0.057 g, 0.26 mmol), and H_2O (30 μL, 1.67 mmol) in DMF (4 mL, 51 mmol) was heated at 130 °C for 48 h. The resulting green powder was then filtered off, washed with DMF, and dried at RT in an air atmosphere. The product was stable in air for 1 d. Compound **2** was analyzed by using a scanning electron microscope (Hitachi S-3400N) and shows typical octahedrally shaped crystals with a size of 10–50 μm (Figure S1 in the Supporting Information). Elemental analysis calcd (%) for $C_{111}H_{143}O_{51}N_{13}U_6$: C 34.1, N 4.7, H 3.7; found: C 35.1, N 4.9, H 3.6.

Compound 3: $[U_6O_4(OH)_4(H_2O)_6(1,4\text{-bdc})_6]\cdot 10\,DMF$ (**3**) was obtained by a solvothermal reaction in which a mixture of UCl_4 (0.1 g, 0.26 mmol), 1,4-H_2bdc (0.043 g, 0.26 mmol), and H_2O (30 μL, 1.67 mmol) in DMF (4 mL, 51 mmol) was heated at 120 °C for 48 h. The resulting green powder was then filtered off, washed with DMF, and dried at RT in an air atmosphere. The product was stable in air for 2–3 d. Compound **3** was analyzed by using a scanning electron microscope (Hitachi S-3400N) and shows typical octahedrally shaped crystals with a size of 10–50 μm (Figure S1 in the Supporting Information). Elemental analysis calcd (%) for $C_{78}H_{110}O_{48}N_{10}U_6$: C 27.7, N 4.1, H 3.2; found: C 27.9, N 3.7, H 3.0.

Compound 4: $[U_6O_4(OH)_4(H_2O)_6(fum)_6]\cdot 5\,DMF$ (**4**) was obtained by a solvothermal reaction in which a mixture of UCl_4 (0.1 g, 0.26 mmol), H_2fum (0.030 g, 0.26 mmol), and H_2O (30 μL, 1.67 mmol) in DMF (4 mL, 51 mmol), heated at 130 °C for 36 h. The resulting green powder was then filtered off, washed with DMF, and dried at RT in an air atmosphere. The product was stable in air for 4–5 d. Compound **4** was analyzed by using a scanning electron microscope (Hitachi S-3400N) and shows typical octahedrally shaped crystals with a size of 5–30 μm (Figure S1 in the Supporting Information). Elemental analysis calcd (%) for $C_{39}H_{47}O_{43}N_5U_6$: C 17.4, N 2.6, H 1.7; found: C 16.2, N 2.2, H 1.9.

Characterization: Crystals were selected and isolated from powdered compounds **1**–**3** by using a polarizing optical microscope and glued on a glass fiber for a single-crystal X-ray diffraction experiment. X-ray intensity data were collected at 100 K (for **1**) or 293 K (for **2**) by using a Bruker X8-APEX2 CCD area-detector diffractometer with $Mo_{K\alpha}$ radiation ($\lambda = 0.71073$ Å) equipped with an optical fiber as collimator. Several sets of narrow data frames (20 s per frame) were collected at different values of θ for two initial values of ϕ and ω, respectively, using 0.3° increments of ϕ or ω. Data reduction was accomplished by using SAINT V7.53a.[27] The substantial redundancy in data allowed a semi-empirical absorption correction (SADABS V2.10) to be applied on the basis of multiple measurements of equivalent reflections. The structure was solved by direct methods, developed by successive difference Fourier syntheses, and refined by full-matrix least-squares on all F data by using the JANA2006 program.[29] The carbon atoms of the benzene rings were refined in two positions due to statistical disorder. The crystal data are given in Table 1.

The pattern of compound **4** (fumarate analog of UiO-66) was scanned at RT by using a Bruker D8 Advance A25 diffractometer with a Debye–Scherrer geometry in the range $2\theta = 5$–110° with a step length of 0.02° (2θ) and a counting time of 3 s step^{-1}. The D8 system was equipped with a LynxEye detector with $Cu_{K\alpha_1/\alpha_2}$ radiation. After data collection, the sta-

Table 1. Crystal data and structure refinement for tetravalent uranium dicarboxylates.

	1	**2**	**3**	**4**
formula	$C_{168}O_{76}U_{12}$	$C_{106}O_{38}U_6$	$C_{68}H_{24}O_{38}U_6$	$C_{54}O_{38}U_6$
M_r	6090.1	3309.3	2877.1	2684.8
T [K]	100	293	293	293
color	green	green	green	green
size [mm]	0.18×0.16×0.09	0.10×0.08×0.07	0.10×0.09×0.06	–
crystal system	cubic	cubic	cubic	cubic
space group	$Fm\bar{3}m$	$F23$	$Fm\bar{3}m$	$P23$
a [Å]	27.4526(9)	24.5681(1)	21.5151(11)	18.7563(3)
V [Å^3]	20689.5(1)	14829.1(1)	9959.3(9)	6598.41(19)
Z	2	4	4	4
ρ_{calcd} [g cm^{-3}]	0.9773	1.4818	1.9182	2.7024
μ [mm^{-1}]	4.717	6.589	9.793	–
ϕ range [°]	1.48–23.49	1.66–31.74	1.64–30.5	5.123–109.996
limiting indices	$-29 \le h \le 29$	$-36 \le h \le 36$	$-30 \le h \le 30$	–
	$-29 \le k \le 29$	$-36 \le k \le 30$	$-14 \le k \le 30$	
	$-29 \le l \le 29$	$-28 \le l \le 36$	$-30 \le l \le 18$	
collected reflns	34981	50459	24013	–
unique reflns	750 [$R_{int}=0.0639$]	4236 [$R_{int}=0.0417$]	826 [$R_{int}=0.0799$]	3312
parameters	22	71	37	179
GOF on F^2	4.34	3.51	2.24	–
Final R indices [$I>2\sigma(I)$]	$R_1=0.0582$	$R_1=0.0592$	$R_1=0.0318$	–
	$wR_2=0.0724$	$wR_2=0.0739$	$wR_2=0.0412$	
R indices (all data)	$R_1=0.0805$	$R_1=0.0896$	$R_1=0.0413$	–
	$wR_2=0.0734$	$wR_2=0.0752$	$wR_2=0.0417$	
Largest diff. peak and hole [e Å^{-3}]	2.46, −1.71	4.09, −2.85	2.04, −1.23	–
R_{WP}	–	–	–	0.119
R_P	–	–	–	0.112
R_{Bragg}	–	–	–	0.0617
R_F	–	–	–	0.0309

bility of the X-ray source and sample was checked by recording the diffraction lines again at low angles. By using DICVOL06 software,[30] a cubic cell with satisfactory figures of merit was found with cell parameters of $a=18.7543$ Å (obtained with the figures of merit $M_{20}=92.0$ and $F_{20}=167.5$ (0.0025, 48)). From the analysis of the available powder data, systematic absences were found to be consistent with the space group $P23$ (no. 195). Structure determination of **4** was carried out by using the parallel tempering algorithm available in the global optimization program FOX.[31] A partial structure was found starting from a unit-cell containing U_6O_8 SBU and six fumarate groups described as a rigid body. The model was completed by Fourier difference analyses. The residue in the cavity was attributed to oxygen atoms. Rietveld refinements were achieved by using FULLPROF.[32] The distances within the fumarate group were restrained to 1.30(2) Å for C2(X)−C2(X), 1.49(2) Å for C1(X)−C2(X), and 1.26(2) Å for C−O within the carboxylate functions. Additionally, soft restrains of 2.67(2) Å were also applied to U−Ow. Final refinements involved the following parameters: atomic coordinates, isotropic atomic displacement parameters, scale factor, zero-point, unit cell parameters, three coefficients for the peak widths, and two line asymmetry parameters. Crystallographic data and details of the Rietveld refinements are given in Table 1. The final Rietveld plot (Figure S3 in the Supporting Information) corresponds to satisfactory model indicators and profile factors (see Table 1).

The thermogravimetric experiments were carried out by using a thermoanalyzer TGA 92 SETARAM under air atmosphere with a heating rate of $5\,^{\circ}C\,min^{-1}$ from RT up to 800 °C. X-ray thermodiffractometry was performed under an air flow of $5\,L\,h^{-1}$ by using an Anton Paar HTK1200N of a D8 Advance Bruker diffractometer (θ–θ mode, $Cu_{K\alpha}$ radiation) equipped with a Vantec1 linear position sensitive detector (PSD). Each powder pattern was recorded in the range of 5–60° (2θ; at intervals of 20 °C up to 800 °C) with a $0.5\,s\,step^{-1}$ scan, which corresponded to an approximate duration of 30 min. The temperature ramps between two patterns were $0.08\,^{\circ}C\,s^{-1}$ up to 600 °C.

The XPS spectrum was collected by using an Axis Ultra DLD (Kratos Analytical) instrument equipped with a monochromatic Al source (1486.69 eV) working at 10 mA and 15 kV with charge compensation.

Infrared analysis was carried out by using a Perkin–Elmer Spectrum 2 instrument equipped with a single reflection diamond module (ATR). IR spectra were recorded in the 400–4000 cm^{-1} range with 4 cm^{-1} resolution.

UV/Vis spectra were collected by using a Perkin–Elmer Lambda 650 spectrophotometer equipped with a powder sample holder set.

Crystallographic data

Data for ***1***: $C_{84}O_{38}U_6$; $M_r=3045.1$; space group $Fm\bar{3}m$, cubic; $a=27.4526(9)$ Å; $V=20689.5(1)$ Å^3; $T=100$ K, $Z=4$; $\mu(Mo_{K\alpha})=4.717$; 34981 reflections measured, 750 independent reflections ($R_{int}=0.0639$); $R_1=(I>2\sigma(I))=0.0582$, $wR_2=0.0724$; GOF = 4.34.

Data for ***2***: $C_{106}O_{38}U_6$; $M_r=3309.3$; space group $F23$, cubic; $a=24.5681(1)$ Å; $V=14829.1(1)$ Å^3; $T=293$ K, $Z=4$; $\mu(Mo_{K\alpha})=6.589$; 50459 reflections measured, 4236 independent reflections ($R_{int}=0.0417$); $R_1=(I>2\sigma(I))=0.0592$, $wR_2=0.0739$; GOF = 3.51.

Data for ***3***: $C_{68}H_{24}O_{24}U_6$; $M_r=2877.1$; space group $Fm\bar{3}m$, cubic; $a=21.5151(11)$ Å; $V=9959.3(9)$ Å^3; $T=293$ K, $Z=4$; $\mu(Mo_{K\alpha})=9.793$; 24013 reflections measured, 826 independent reflections ($R_{int}=0.0799$); $R_1=(I>2\sigma(I))=0.0318$, $wR_2=0.0412$; GOF = 2.24.

Data for ***4***: $C_{54}O_{38}U_6$; $M_r=2684.8$; space group $P23$, cubic; $a=18.7563(3)$ Å; $V=6598.41(19)$ Å^3; $T=293$ K, $Z=4$; 3312 reflections measured, $R_{WP}=0.119$, $R_P=0.112$; $R_{Bragg}=0.0617$, $R_F=0.0309$.

CCDC-906871 (**1**), CCDC-906872 (**2**) and CCDC-906873 (**3**) contain the supplementary crystallographic data for this paper. These data can be obtained free of charge from The Cambridge Crystallographic Data Centre via www.ccdc.cam.ac.uk/data_request/cif.

Acknowledgements

The authors would like to thank the GNR MATINEX of PACEN interdisciplinary program and the French ANR project no. ANR-08-BLAN-0216-01 for financial support. The authors also thank Prof. Marc Visseaux for help with the synthesis of UCl_4 and Prof. Francis Abraham for helpful discussions, Mrs. Nora Djelal and Laurence Burylo for their technical assistance with the SEM images, TG measurements, and powder XRD (UCCS). The Fonds Européen de Développement Régional (FEDER), the CNRS, the Région Nord Pas-de-Calais, and the Ministère de l'Education Nationale de l'Enseignement Supérieur et de la Recherche are acknowledged for funding of the X-ray diffractometers. C.F. acknowledges Université Lille 1 and Région Nord Pas-de-Calais for PhD grant support.

[1] P. C. Burns, *Can. Mineral.* **2005**, *43*, 1839.
[2] a) M. C. Favas, D. L. Kepert, J. M. Patrick, A. H. White, *J. Chem. Soc. Dalton Trans.* **1983**, 571; b) M. R. Spirlet, J. Rebizant, B. Kanellakopulos, E. Dornberger, *J. Less-Common Met.* **1986**, *122*, 205; c) K. P. Mörtl, J.-P. Sutter, S. Golhen, L. Ouahab, O. Kahn, *Inorg. Chem.* **2000**, *39*, 1626; d) I. Imaz, G. Bravic, J.-P. Sutter, *Dalton Trans.* **2005**, 2681; e) B. Chapelet-Arab, G. Nowogrocki, F. Abraham, S. Grandjean, *J. Solid State Chem.* **2005**, *178*, 3046; f) B. Chapelet-Arab, G. Nowogrocki, F. Abraham, S. Grandjean, *J. Solid State Chem.* **2005**, *178*, 3055; g) B. Chapelet-Arab, L. Duvieubourg, G. Nowogrocki, F. Abraham, S. Grandjean, *J. Solid State Chem.* **2006**, *179*, 4029; h) B. Arab-Chapelet, S. Grandjean, G. Nowogrocki, F. Abraham, *J. Alloys Compd.* **2007**, *444–445*, 387; i) B. Arab-Chapelet, S. Grandjean, G. Nowogrocki, F. Abraham, *J. Nucl. Mater.* **2008**, *373*, 259; j) L. Duvieubourg-Garela, N. Vigier, F. Abraham, S. Grandjean, *J. Solid State Chem.* **2008**, *181*, 2008; k) C.-M. Wang, C.-H. Liao, P.-L. Chen, K.-H. Lii, *Inorg. Chem.* **2006**, *45*, 1436; l) C.-M. Wang, Y.-Y. Wu, P.-L. Chen, K.-H. Lii, *Dalton Trans.* **2007**, 1034; m) N. Clavier, N. Hingant, M. Rivenet, S. Obbade, N. Dacheux, N. Barré, F. Abraham, *Inorg. Chem.* **2010**, *49*, 1921; n) G. Andreev, N. Budantseva, A. Fedoseev, P. Moisy, *Inorg. Chem.* **2011**, *50*, 11481.
[3] a) J. Leciejewicz, N. W. Alcock, T. J. Kemp, *Struct. Bonding (Berlin)* **1995**, *82*, 43; b) C. L. Cahill, D. T. de Lill, M. Frisch, *CrystEngComm* **2007**, *9*, 15; c) K.-X. Wang, J.-S. Chen, *Acc. Chem. Res.* **2011**, *44*, 531; d) P. Thuéry, B. Masci, *CrystEngComm* **2012**, *14*, 131; e) I. Mihalcea, N. Henry, C. Volkringer, T. Loiseau, *Cryst. Growth Des.* **2012**, *12*, 526.
[4] Special issue on MOFs: Guest Editors: H.-C. Zhou, J. R. Long, O. M. Yaghi, *Chem. Rev.* **2012**, *112*, 673.
[5] a) R. C. Paul, J. S. Ghotra, M. S. Bains, *J. Inorg. Nucl. Chem.* **1965**, *27*, 265; b) I. Jelenic, D. Grdenic, A. Bezjak, *Acta Crystallogr.* **1964**, *17*, 758.
[6] a) Y.-J. Zhang, D. Collison, F. R. Livens, A. K. Powell, S. Wocadlo, H. Eccles, *Polyhedron* **2000**, *19*, 1757; b) G. J. Vazquez, C. J. Dodge, A. J. Francis, *Inorg. Chem.* **2009**, *48*, 9485; c) S. Takao, K. Takao, W. Kraus, F. Emmerling, A. C. Scheinost, G. Bernhard, C. Hennig, *Eur. J. Inorg. Chem.* **2009**, 4771; d) V. Mougel, B. Biswas, J. Pécaut, M. Mazzanti, *Chem. Commun.* **2010**, *46*, 8648; e) B. Biswas, V. Mougel, J. Pécaut, M. Mazzanti, *Angew. Chem.* **2011**, *123*, 5863; *Angew. Chem. Int. Ed.* **2011**, *50*, 5745; f) K. E. Knope, L. Soderholm, *Chem. Rev.* **2013**, *113*, dx.doi.org/10.1021/cr300212f.
[7] G. Nocton, F. Burdet, J. Pécaut, M. Mazzanti, *Angew. Chem.* **2007**, *119*, 7718; *Angew. Chem. Int. Ed.* **2007**, *46*, 7574.
[8] C. Volkringer, I. Mihalcea, J.-F. Vigier, A. Beaurain, M. Visseaux, T. Loiseau, *Inorg. Chem.* **2011**, *50*, 11865.
[9] J. Hafizovic Cavka, S. Jakobsen, U. Olsbye, N. Guilou, C. Lamberti, S. Bordiga, K. P. Lillerud, *J. Am. Chem. Soc.* **2008**, *130*, 13850.
[10] G. Wissmann, A. Schaate, S. Lilienthal, I. Bremer, A. M. Schneider, P. Behrens, *Mic. Mes. Mater.* **2012**, *152*, 64.
[11] G. Lundgren, *Arkiv Kemi* **1953**, *5*, 349.
[12] L. M. Mokry, N. S. Dean, C. J. Carrano, *Angew. Chem.* **1996**, *108*, 1676; *Angew. Chem. Int. Ed. Engl.* **1996**, *35*, 1497.

[13] J.-C. Berthet, P. Thuéry, M. Ephritikhine, *Chem. Commun.* **2005**, 3415.
[14] a) J.-H. Liu, S. Van den Berghe, M. J. Konstantinovic, *J. Solid State Chem.* **2009**, *182*, 1105; b) H.-K. Liu, K.-H. Lii, *Inorg. Chem.* **2011**, *50*, 5870; c) C.-S. Lee, S.-L. Wang, K.-H. Lii, *J. Am. Chem. Soc.* **2009**, *131*, 15116.
[15] a) J. G. Conway, *J. Chem. Phys.* **1959**, *31*, 1002; b) D. Cohen, W. T. Carnall, *J. Phys. Chem.* **1960**, *64*, 1933; c) S. Hubert, C. L. Song, M. Genet, F. Auzel, *J. Solid State Chem.* **1986**, *61*, 252; d) N. Dacheux, V. Brandel, M. Genet, *New J. Chem.* **1995**, *19*, 15.
[16] M. L. Foo, S. Horike, T. Fukushima, Y. Hijikata, Y. Kubota, M. Takata, S. Kitagawa, *Dalton Trans.* **2012**, *41*, 13791.
[17] V. Guillerm, S. Gross, C. Serre, T. Devic, M. Bauer, G. Férey, *Chem. Commun.* **2010**, *46*, 767.
[18] A. Schaate, P. Roy, A. Godt, J. Lippke, F. Waltz, M. Wiebke, P. Behrens, *Chem. Eur. J.* **2011**, *17*, 6643.
[19] A. Schaate, S. Dühnen, G. Platz, S. Lilienthal, A. M. Schneider, P. Behrens, *Eur. J. Inorg. Chem.* **2012**, 790.
[20] a) W. Morris, B. Volosskiy, S. Demir, F. Gandara, P. L. McGrier, H. Furukawa, D. Cascio, J. F. Stoddart, O. M. Yaghi, *Inorg. Chem.* **2012**, *51*, 6443; b) V. Bon, V. Senkovskyy, I. Senkovska, S. Kaskel, *Chem. Commun.* **2012**, *48*, 8407.
[21] a) G. Kickelbick, U. Schubert, *Chem. Ber.* **1997**, *130*, 473; b) G. Kickelbick, P. Wiede, U. Schubert, *Inorg. Chim. Acta* **1999**, *284*, 1.
[22] a) P. Toledano, F. Ribot, C. Sanchez, *C. R. Acad. Sci. Ser. II* **1990**, *311*, 1315; b) V. Mereacre, M. N. Akhtar, A. Lindemann, C. E. Anson, A. K. Powell, *Helv. Chim. Acta* **2009**, *92*, 2507.
[23] a) K. E. Knope, R. E. Wilson, M. Viasiliu, D. A. Dixon, L. Soderholm, *Inorg. Chem.* **2011**, *50*, 9696; b) C. Hennig, S. Takao, K. Takao, S. Weiss, W. Kraus, F. Emmerling, A. C. Scheinost, *Dalton Trans.* **2012**, *41*, 12818.
[24] P. B. Duval, C. J. Burns, D. L. Clark, D. E. Morris, B. L. Scott, J. D. Thompson, E. L. Werkema, L. Jia, R. A. Andersen, *Angew. Chem.* **2001**, *113*, 3461; *Angew. Chem. Int. Ed.* **2001**, *40*, 3357.
[25] J. Diwu, S. Wang, T. E. Albrecht-Schmitt, *Inorg. Chem.* **2012**, *51*, 4088.
[26] K. Takao, S. Takao, A. C. Scheinost, G. Bernhard, C. Hennig, *Inorg. Chem.* **2012**, *51*, 1336.
[27] SAINT Plus, Version 7.53 a, Bruker Analytical X-ray Systems, Madison, WI, **2008**.
[28] G. M. Sheldrick, SADABS, Version 2008/1, Bruker-Siemens Area Detector Absorption and Other Correction, **2008**.
[29] V. Petricek, M. Dusek, L. Palatinus, JANA2006, Institute of Physics, Praha, **2006**.
[30] D. Louër, A. Buoltif, *Z. Kristallogr.* **2007**, *26*, 191.
[31] V. Favre-Nicolin, R. Cerny, *J. Appl. Crystallogr.* **2002**, *35*, 734.
[32] J. Rodriguez-Carvajal, *Physica B* **1993**, *192*, 55.

Received: November 1, 2012
Published online: January 16, 2013

